PHYSICAL REVIEW D **91,** 055026 (2015)

Low-energy phenomenology of trinification: An effective left-right-symmetric model

Jamil Hetzel[*] and Berthold Stech[†]

Institut für Theoretische Physik, Universität Heidelberg, D-69120 Heidelberg, Germany

(Received 9 February 2015; published 25 March 2015)

The trinification model is an interesting extension of the Standard Model (SM) based on the gauge group $SU(3)_C \times SU(3)_L \times SU(3)_R$. We study its low-energy phenomenology by constructing a low-energy effective field theory, thereby reducing the number of particles and free parameters that need to be studied. The resulting model predicts that several new scalar particles have masses in the $\mathcal{O}(100\ \mathrm{GeV})$ range. We study a few of the interesting phenomenological scenarios, such as the presence of a light fermiophobic scalar in addition to a SM-like Higgs, or a degenerate (twin) Higgs state at 126 GeV. We point out regions of the parameter space that lead to measurable deviations from SM predictions of the Higgs couplings. Hence, the trinification model awaits crucial tests at the Large Hadron Collider in the coming years.

DOI: 10.1103/PhysRevD.91.055026 PACS numbers: 12.10.Dm

I. INTRODUCTION

The discovery of the Higgs boson [1,2] marks the establishment of the Standard Model (SM) of particle physics as the model that correctly describes physics at experimentally available energies to date. All SM particles have been discovered, and the experimental data gathered at particle colliders match the predictions of the SM to good precision [3]. Yet, the SM is regarded as an incomplete theory of nature: it lacks a dark matter candidate and is incompatible with the observation of nonzero neutrino masses. Also, the fermion masses and mixings are free parameters that display hierarchical patterns, and parity violation is introduced by hand. Therefore, our quest towards a better theory of nature requires us to extend the SM.

Grand unified theories (GUTs) [4–8] are interesting extensions of the SM in which the SM gauge group $SU(3)_C \times SU(2)_L \times U(1)_Y$ is embedded in a larger simple gauge group. The exceptional group E_6 is an attractive example of a GUT group [6–8]. It is anomaly free and left-right-symmetric (LR-symmetric), and as such it provides an explanation for parity violation in the SM by spontaneous symmetry breaking. It appears in the compactification of string theories, which leads to either four-dimensional E_6 gauge symmetry or one of E_6's maximal subgroups [9,10]. One of these maximal subgroups is the "trinification group" $G_{333} \equiv SU(3)_C \times SU(3)_L \times SU(3)_R$. Models based on the trinification group have been studied in several contexts [11–18].

In this work, "trinification model" will refer to the setup described in Refs. [7,19–23]. The setup described there is interesting for several reasons: fermion masses and mixings of the SM can be reproduced using only a few parameters, with a satisfactory fit for the solar neutrino mass difference and the neutrino mixing pattern. Also, a Standard-Model-like Higgs with a mass close to 126 GeV appears in a large region of parameter space of the model. Furthermore, it gives predictions for the matrix element of neutrinoless double-beta decay and the neutrino masses, which allow the model to be tested with low-energy experiments. It also allows for various interesting phenomenological scenarios, such as the presence of a light fermiophobic Higgs in addition to the Standard-Model-like Higgs, or even a degenerate Higgs state at 126 GeV.

In order to compare the trinification model with experiment, a study of the low-energy phenomenology is necessary. Due to the large number of scalars, a study of the full scalar mass matrix is challenging. However, several of the scalar fields will obtain very large masses when the trinification symmetry is broken, and thus can be integrated out from the theory. The result is an effective field theory with the LR-symmetric gauge group $SU(3)_C \times SU(2)_L \times SU(2)_R \times U(1)_{B-L}$, and fewer scalar fields than in the trinification model. This model has the same low-energy properties as the trinification model but is easier to study. We will refer to this model as the low-energy trinification (LET) model.

Neither the LET model nor the trinification model resolves the hierarchy problem. This problem is hidden in the vacuum expectation values (VEVs) used in the model, which are presently not understood. In our treatment, all dimensionful parameters and masses are fully determined by these VEVs multiplied by dimensionless coupling constants. Since these VEVs are momentum and scale independent (except for wave-function renormalization), their use as fixed parameters is justified.

Left-right symmetric models based on the gauge group $SU(3)_C \times SU(2)_L \times SU(2)_R \times U(1)_{B-L}$ [24–26] have been studied extensively in the literature. Moreover, these models have many features in common with the two-Higgs-doublet model (2HDM) [27]. However, the LET

[*]hetzel@thphys.uni-heidelberg.de
[†]b.stech@thphys.uni-Heidelberg.de

 © 2015 American Physical Society

model has properties that distinguish it from more general LR-symmetric models and the 2HDM, due to the trinification origin at high energy scales. A LR-symmetric model in the context of the trinification model has not been studied before to the best of our knowledge. Therefore, the LET model merits a study.

In this work, we explore the low-energy phenomenology of the LET model. We briefly describe the trinification model in Sec. II, and subsequently derive the properties of the LET model in Sec. III. In order to aid our study of the LET model, we first introduce the single-bidoublet (SB) model, a simplified form of the LET model that has fewer scalar fields. The possible phenomenological scenarios for both the SB model and the LET model are worked out in Sec. IV. We show how these models may be distinguished experimentally from the SM by studying the modifications of the SM Higgs couplings in Sec. V. It turns out that the LET model allows for interesting phenomenological scenarios, such as a very light fermiophobic scalar with a mass in the GeV range or a degenerate scalar state at 126 GeV. We discuss these scenarios in more detail in Secs. VI and VII. Our conclusions are presented in Sec. VIII.

II. THE TRINIFICATION MODEL

The Higgs sector of the trinification model contains two complex scalar fields H_1, H_2 in the $(\mathbf{1}, \bar{\mathbf{3}}, \mathbf{3})$ representation of $G_{333} \equiv SU(3)_C \times SU(3)_L \times SU(3)_R$. We can use the $SU(3)_L \times SU(3)_R$ gauge symmetry to bring the VEV of H_1 into diagonal form:

$$\langle H_1 \rangle = \frac{1}{\sqrt{2}} \begin{pmatrix} v_1 & 0 & 0 \\ 0 & b_1 & 0 \\ 0 & 0 & M_1 \end{pmatrix},$$
$$\langle H_2 \rangle = \frac{1}{\sqrt{2}} \begin{pmatrix} v_2 & 0 & 0 \\ 0 & b_2 & b_3 \\ 0 & M & M_2 \end{pmatrix}. \tag{1}$$

Here we employed a matrix notation in which $SU(3)_L$ indices run vertically and $SU(3)_R$ indices run horizontally. All VEV parameters are taken to be real in order to avoid tree-level CP-violation. The second field H_2 is necessary to break the left-right symmetry of G_{333}: it cannot be made diagonal once $\langle H_1 \rangle$ is taken to be diagonal. The off-diagonal parameters M, b_3 are taken to be unequal, and thus break the left-right symmetry. We assume the presence of large hierarchies among the VEV parameters. The parameters $M_1, M_2 \sim 10^{13}$ GeV are of the order of the scale where the Standard Model gauge couplings g_1 and g_2 unify. The off-diagonal VEV M is taken to be an intermediate scale of order 10^{10} GeV, but could also be as low as a few TeV. The gauge couplings $g_{L,R}$ of $SU(3)_{L,R}$ are equal above this scale, whereas below M the left-right symmetry is broken. The other VEV parameters contribute to the W-boson mass and are, therefore, much smaller than M_1, M_2, M. As such, the former are constrained by the relation $v_1^2 + v_2^2 + b_1^2 + b_2^2 + b_3^2 = v^2 = (246\ \text{GeV})^2$. The used scalar potential is renormalizable and all its parameters are taken to be real in order to avoid tree-level CP-violation.

The fermions are grouped into the fundamental representation **27** of E_6. They are two-component left-handed Weyl spinors with respect to the Lorentz group. The fermion field decomposes into a lepton field L, a left-handed quark field Q_L, and a right-handed quark field Q_R, which are assigned to the representations of $SU(3)_C \times SU(3)_L \times SU(3)_R$ as follows:

$$L \sim (\mathbf{1}, \bar{\mathbf{3}}, \mathbf{3}), \qquad Q_L \sim (\bar{\mathbf{3}}, \mathbf{3}, \mathbf{1}), \qquad Q_R \sim (\mathbf{3}, \mathbf{1}, \bar{\mathbf{3}}). \tag{2}$$

In matrix notation, L is a 3×3 matrix, Q_L is a column vector, and Q_R is a row vector:

$$L = \begin{pmatrix} L_1^1 & E^- & e^- \\ E^+ & L_2^2 & \nu \\ e^+ & \hat{\nu} & L_3^3 \end{pmatrix},$$
$$Q_L^b = \begin{pmatrix} u^b \\ d^b \\ D^b \end{pmatrix}, \qquad Q_R^b = \begin{pmatrix} \hat{u}^b & \hat{d}^b & \hat{D}^b \end{pmatrix}. \tag{3}$$

Here $b = 1, 2, 3$ is a color index. The components u, d are the left-handed up-type and down-type quarks from the SM, whereas D is a new quark with electromagnetic charge $-\frac{1}{3}$. The components $\hat{u}$, $\hat{d}$, $\hat{D}$ are their respective right-handed counterparts. The lepton field contains the charged leptons $e^\pm$ and the left-handed neutrino ν. It contains several new states: a right-handed neutrino $\hat{\nu}$; three neutral states L_1^1, L_2^2, L_3^3; and a pair of charged leptons $E^\pm$. A generation index $\alpha = 1, 2, 3$ on the fermion fields in Eq. (3) has been suppressed.

The Higgs fields H_1, H_2 cannot both couple to fermions, since this would lead to flavor-changing neutral current (FCNC) processes, which are severely restricted by experiment. In order to suppress tree-level FCNC interactions, the existence of a Z_2 symmetry is assumed under which H_1 (H_2) is even (odd). The fermions are even under this symmetry as well, which implies that H_2 does not couple to fermions. The Yukawa couplings are of the form

$$\begin{aligned} \mathcal{L}_Y = &-g_t G_{\alpha\beta} \left(Q_R^\alpha H_1^T Q_L^\beta + \frac{1}{2} \epsilon^{ijk} \epsilon_{lmn} L_l^i L_m^j (H_1)_n^k \right) \\ &- A_{\alpha\beta} (Q_R^\alpha H_{Aq}^T Q_L^\beta + \epsilon^{ijk} L_l^i L_m^j (H_{Al})_{\{lm\}}^k) \\ &- \frac{1}{M_N} (G^2)_{\alpha\beta} \mathrm{Tr}\{L^\alpha H_1^\dagger\} \mathrm{Tr}\{H_2^\dagger L^\beta\} + \text{H.c.} \end{aligned} \tag{4}$$

The first line is a Yukawa interaction built from the fields we have already introduced: the parameter g_t is a dimensionless coupling, $G_{\alpha\beta}$ is a symmetric 3×3 generation matrix, and ϵ is a totally antisymmetric symbol with $\epsilon^{123}=\epsilon_{123}=+1$. This interaction is sufficient to reproduce the up-quark masses by choosing a generation basis in which $g_t G_{\alpha\beta}$ is diagonal and fitting its diagonal components to the up-quark masses [23]. The VEV M_1 in Eq. (1) gives large masses to D, $E^{\pm}$. The second line in Eq. (4) contains interactions with new scalar fields $H_{Aq}\sim(\mathbf{1},\bar{\mathbf{3}},\mathbf{3})$ and $H_{Al}\sim(\mathbf{1},\bar{\mathbf{3}},\bar{\mathbf{6}})$, coupling to the fermions with a Hermitian antisymmetric matrix $A_{\alpha\beta}$. [28] These terms come from the couplings of a scalar field H_A in the antisymmetric $\mathbf{351_A}$ representation of E_6. This interaction is necessary to describe the masses and mixings of the down quarks and charged leptons correctly: the Standard Model down quarks and charged leptons are mixed with their heavy partners via the seesaw mechanism. A good fit for the masses and mixings of the Standard Model fermions is obtained using only very few extra parameters [23]. It is assumed that the fields H_{Aq}, H_{Al} have negligible mixing with H_1, H_2 in order to simplify the analysis of the scalar spectrum.

At this stage, neutrinos are still Dirac particles with masses comparable to the other fermion masses. The third line in Eq. (4) is necessary to obtain neutrino masses in accordance with experiment. This line contains an effective dimension-five Yukawa interaction that could originate from the exchange of a new heavy Dirac fermion that is a trinification singlet [20]. It violates the Z_2 symmetry and mixes the neutrinos ν, $\hat{\nu}$ with the other neutral leptons L_1^1, L_2^2, L_3^3, giving rise to a generalized seesaw mechanism. The light-neutrino mass matrix introduces two additional parameters, which can be fixed by the experimentally observed atmospheric mass-squared difference and the lightest neutrino mass [23].

III. AN EFFECTIVE TRINIFICATION MODEL: THE LET MODEL

We now consider the effective trinification model obtained after integrating out the Higgs fields that are made heavy by the large VEVs M_1 and M_2. We expect the Higgs fields that are right-handed singlets with respect to the SM to obtain large masses. These are the fields with the $SU(3)_R$ index (3). On the other hand, the fields (3,1) and (3,2) of H_2 that are left-handed singlets (with respect to the SM) are kept. These Higgs fields are necessary to describe the breaking of the left-right symmetry. The corresponding scale M is certainly larger than the weak scale, but may be much lower than M_1 and M_2.

The 2×2 blocks in the upper left corners of the fields H_1, H_2 transform as bidoublets $\Phi_1,\Phi_2\sim(\mathbf{1},\bar{\mathbf{2}},\mathbf{2},0)$ under $SU(3)_C\times SU(2)_L\times SU(2)_R\times U(1)_{B-L}$. The (3,1) and (3,2) components of H_2 transform as a right-handed doublet $\Phi_R\sim(\mathbf{1},\mathbf{1},\mathbf{2},1)$:

$$\Phi_i=\begin{pmatrix}\Phi^0_{i,11} & \Phi^-_{i,21}\\ \Phi^+_{i,12} & \Phi^0_{i,22}\end{pmatrix}\leftrightarrow\begin{pmatrix}(H_i)^1_1 & (H_i)^1_2 & 0\\ (H_i)^2_1 & (H_i)^2_2 & 0\\ 0 & 0 & 0\end{pmatrix},$$
$$\Phi_R=\begin{pmatrix}\Phi^+_R & \Phi^0_R\end{pmatrix}\leftrightarrow\begin{pmatrix}0 & 0 & 0\\ 0 & 0 & 0\\ (H_2)^3_1 & (H_2)^3_2 & 0\end{pmatrix}. \quad (5)$$

These fields obtain the following VEVs:

$$\langle\Phi_i\rangle=\frac{1}{\sqrt{2}}\begin{pmatrix}v_i & 0\\ 0 & b_i\end{pmatrix},$$
$$\langle\Phi_R\rangle=\frac{1}{\sqrt{2}}\begin{pmatrix}0 & M\end{pmatrix}. \quad (6)$$

The fields Φ_1, Φ_2, Φ_R, and their VEVs are sufficient to describe the symmetry breaking from $SU(3)_C\times SU(2)_L\times SU(2)_R\times U(1)_{B-L}$ to electromagnetism via the SM. Note that a right-handed doublet like Φ_R resides in H_1 as well. In principle, Φ_R may be a combination of both. Note that the (3,3) components of H_1 and H_2 are total gauge singlets. A combination of them, if sufficiently light, could be a dark matter candidate. Also note that Φ_2 and Φ_R do not couple to fermions.

Besides the eight gluon fields of $SU(3)_C$, the gauge-boson sector consists of seven vector gauge bosons. Their masses and mixings are given in Sec. A. The VEVs of $\Phi_{1,2}$ contribute to the W mass and are, therefore, constrained by the relation $v_1^2+b_1^2+v_2^2+b_2^2=v^2=(246\ \mathrm{GeV})^2$. It is convenient to reparametrize the VEV parameters as

$$v_1=v\cos\alpha\cos\beta_1,$$
$$v_2=v\sin\alpha\cos\beta_2,$$
$$b_1=v\cos\alpha\sin\beta_1,$$
$$b_2=v\sin\alpha\sin\beta_2. \quad (7)$$

The parameter M is a mass scale above the electroweak scale. Because of this hierarchy, it will often be convenient to use the small parameter $\xi\equiv v/M$.

We build the scalar potential of the LET model from all possible gauge-invariant renormalizable operators consisting of Φ_1, Φ_2, Φ_R, leaving out those that could not have arisen from the trinification model. This means that we do not include operators involving charge conjugates: since the $\mathbf{3}$ and $\bar{\mathbf{3}}$ representations of $SU(3)$ are inequivalent, such operators have no possible origin in the trinification model. The resulting potential is

$$
\begin{aligned}
V &= V_1(\Phi_1,\Phi_R) + V_2(\Phi_1,\Phi_2,\Phi_R),\\
V_1 &= \frac{\lambda_1}{2}\mathrm{Tr}\{\Phi_1^\dagger\Phi_1\}^2 + \frac{\lambda_2}{2}\mathrm{Tr}\{\Phi_1^\dagger\Phi_1\Phi_1^\dagger\Phi_1\} + \frac{\lambda_3}{2}(\Phi_R\Phi_R^\dagger)^2 + \lambda_4\mathrm{Tr}\{\Phi_1^\dagger\Phi_1\}(\Phi_R\Phi_R^\dagger) + \lambda_5\Phi_R\Phi_1^\dagger\Phi_1\Phi_R^\dagger + \mu_{11}^2\mathrm{Tr}\{\Phi_1^\dagger\Phi_1\}\\
&\quad + \mu_R^2\Phi_R\Phi_R^\dagger + (\mu_1^2\det\Phi_1 + \mathrm{H.c.}),\\
V_2 &= \frac{\tilde\lambda_1}{2}\mathrm{Tr}\{\Phi_2^\dagger\Phi_2\}^2 + \frac{\tilde\lambda_2}{2}\mathrm{Tr}\{\Phi_2^\dagger\Phi_2\Phi_2^\dagger\Phi_2\} + \tilde\lambda_3\mathrm{Tr}\{\Phi_2^\dagger\Phi_2\}(\Phi_R\Phi_R^\dagger) + \tilde\lambda_4\Phi_R\Phi_2^\dagger\Phi_2\Phi_R^\dagger + \tilde\lambda_5\mathrm{Tr}\{\Phi_1^\dagger\Phi_1\}\mathrm{Tr}\{\Phi_2^\dagger\Phi_2\}\\
&\quad + \tilde\lambda_6|\mathrm{Tr}\{\Phi_1^\dagger\Phi_2\}|^2 + \frac{\tilde\lambda_7}{2}(\mathrm{Tr}\{\Phi_1^\dagger\Phi_2\}^2 + \mathrm{H.c.}) + \tilde\lambda_8\mathrm{Tr}\{\Phi_1^\dagger\Phi_1\Phi_2^\dagger\Phi_2\} + \tilde\lambda_9\mathrm{Tr}\{\Phi_1^\dagger\Phi_2\Phi_2^\dagger\Phi_1\}\\
&\quad + \frac{\tilde\lambda_{10}}{2}(\mathrm{Tr}\{\Phi_1^\dagger\Phi_2\Phi_1^\dagger\Phi_2\} + \mathrm{H.c.}) + \mu_{22}^2\mathrm{Tr}\{\Phi_2^\dagger\Phi_2\} + (\mu_2^2\det\Phi_2 + \mathrm{H.c.}).
\end{aligned}
\tag{8}
$$

For later convenience, we have split the potential into the parts V_1 and V_2 that, respectively, do and do not depend on Φ_2. As mentioned in the introduction, the five dimensionful parameters μ_{11}^2, μ_{22}^2, μ_R^2, μ_1^2, μ_2^2 are no free parameters. They are determined in terms of the VEV parameters v_1, b_1, v_2, b_2, M and the dimensionless parameters λ_i, $\tilde\lambda_j$ by the requirement that V has an extremum at the appropriate place.

In the trinification model, the fermions obtain their masses from Yukawa interactions with H_1. In order to combine the leptons and Φ_1 into a gauge singlet, we need the antisymmetric tensor $i\sigma_2$, which can be absorbed into a redefinition of the lepton fields. Absorbing a minus sign into the phase of the $e^\pm$ fields, the fermionic field content of the LET model becomes

$$
\begin{aligned}
Q_L &\equiv \begin{pmatrix} u \\ d \end{pmatrix} \sim \left(\bar{\mathbf{3}}, \mathbf{2}, \mathbf{1}, \frac{1}{3}\right),\\
Q_R &\equiv \begin{pmatrix} \hat u & \hat d \end{pmatrix} \sim \left(\mathbf{3}, \mathbf{1}, \bar{\mathbf{2}}, -\frac{1}{3}\right),\\
L^- &\equiv \begin{pmatrix} \nu \\ e^- \end{pmatrix} \sim (\mathbf{1}, \mathbf{2}, \mathbf{1}, -1),\\
L^+ &\equiv \begin{pmatrix} \hat\nu & e^+ \end{pmatrix} \sim (\mathbf{1}, \mathbf{1}, \bar{\mathbf{2}}, 1).
\end{aligned}
\tag{9}
$$

After integrating out the heavy fields, the first line of the Yukawa Lagrangian in Eq. (4) becomes

$$
\mathcal{L}_Y = -G_{\alpha\beta}(Q_R^\alpha\Phi_1^T Q_L^\beta + L^{+\alpha}\Phi_1^T L^{-\beta}) + \mathrm{H.c.} \tag{10}
$$

This term is insufficient to describe all fermion masses correctly: down-quark masses as well as the charged-lepton and neutrino masses would be proportional to each other and the CKM matrix would be a unit matrix at this point. In order to describe the fermion masses and mixings correctly, interactions with the additional fields H_{Aq}, H_{Al} need to be included. Here we restrict ourselves to the single Yukawa term in Eq. (10) and fit the free parameters to the top- and bottom-quark masses: these fermions are the most relevant to compare our analysis to experimental searches for new physics. We assume that flavor physics for the lower fermion masses does not influence the spectrum of the scalar particles. Fitting the free parameters to the top- and bottom-quark masses, we find $v = 246$ GeV, $\tan\beta_1 = m_b/m_t \Rightarrow \beta_1 = 0.0166$. Since Φ_2 does not contribute to the fermion masses, we have no such restrictions on β_2 and α.

A. The single-bidoublet model

The scalar potential of the LET model in Eq. (8) contains 15 free coupling constants, which are difficult to deal with. As an intermediate step towards an understanding of the LET model, we first discuss a model from which Φ_2 has been omitted; we will refer to this setup as the single-bidoublet (SB) model. This model corresponds to the LET-model limit $\alpha = 0$, $\mu_{22}^2 \to \infty$ ($\alpha = 0$ implies $v_2 = b_2 = 0$, for which μ_{22}^2 is no longer constrained by the location of the minimum of the scalar potential). Note however that the SB model is not an appropriate effective field theory of the trinification model, since the VEV parameters of Φ_2 are of order v for the general case $\alpha \neq 0$. Rather, we use it as a toy model that helps us study the phenomenology of the LET model.

The most general scalar potential for the SB model is given by $V_1(\Phi_1,\Phi_R)$ in Eq. (8). The minimalization of this potential at the VEV in Eq. (6) fixes the dimensionful parameters μ_{11}^2, μ_R^2, μ_1^2 in terms of the λ_i and the VEV parameters v_1, b_1, M. The VEV parameters v_1, b_1 can be reparametrized in terms of v, β_1 by Eq. (7), with $\alpha = 0$.

The scalar fields Φ_1, Φ_R contain twelve real scalar components in total. After spontaneous symmetry breaking, six of them become massless Goldstone bosons that give mass to the six massive vector gauge bosons. The remaining components mix to form six massive scalars: three CP-even scalars h^0, H_1^0, and H_2^0, one CP-odd scalar A^0, and a pair of charged scalars $H^\pm$. Their definitions in terms of gauge eigenstates as well as their masses are given in Sec. B. We identify h^0 with the Standard-Model-like Higgs particle that has been observed at the LHC [1,2],

since it is the only scalar that naturally has a mass at the electroweak scale. The other scalars have masses of order M unless we give $\mathcal{O}(\xi^2) = \mathcal{O}(v^2/M^2)$ values to some of the dimensionless scalar-potential parameters.

Note that the SB model resembles the two-Higgs-doublet model (2HDM) [27] (see [29] for a recent review). The 2HDM is an extension of the SM in which the scalar sector contains an additional $SU(2)_L$ doublet. It has been studied extensively since it provides a low-energy description of various models such as supersymmetry (see e.g. [30] for a review), composite Higgs models [31], and little Higgs models [32].

It is easy to see why the SB model resembles the 2HDM at the Lagrangian level. To this end, we write $\Phi_1 = (i\sigma_2\phi_1, \phi_2^*)$ and $\Phi_R = (\phi_+, \phi_0)$, where $\phi_{1,2}$ are $SU(2)_L$ doublets and $\phi_{+,0}$ are $SU(2)_L$ singlets. Since Φ_R has a much larger VEV M than the VEV components v_1, b_1 of Φ_1, the mixing among Φ_1, Φ_R will be of order $\xi \ll 1$. If we set $\Phi_R = 0$ in the scalar potential V_1 in Eq. (8), we can rewrite the entire scalar potential in terms of ϕ_1, ϕ_2 only. The result is a 2HDM potential (see e.g. Eq. (98) in Ref. [29]) with the following constraints on the scalar parameters:

$$\lambda_{1,2,3}^{\mathrm{2HDM}} = \lambda_1 + \lambda_2, \qquad \lambda_4^{\mathrm{2HDM}} = -\lambda_2, \qquad \lambda_{5,6,7}^{\mathrm{2HDM}} = 0,$$
$$m_{11}^2 = m_{22}^2 = \mu_{11}^2, \qquad m_{12}^2 = -\mu_1^2. \tag{11}$$

We can rewrite the Yukawa sector of the LET model in terms of ϕ_1, ϕ_2 as well. In the Lagrangian in Eq. (10), the up-type fermions couple only to ϕ_1 whereas the down-type fermions couple only to ϕ_2. Hence, the SB model resembles a constrained type-II 2HDM setup. It differs from the 2HDM due to the presence of two additional heavy $SU(2)_L$ singlets. The neutral one gives rise to an additional physical particle H_2^0 that is fermiophobic. Its mass can be tuned independently from the masses of the 2HDM-like scalars H_1^0, A^0, $H^\pm$ [see Eq. (B2)]. This can result in phenomenological scenarios that cannot appear in the 2HDM. Moreover, the VEV ratio $\tan\beta \equiv \langle\phi_2\rangle/\langle\phi_1\rangle$ is a free parameter in the 2HDM, whereas $\tan\beta_1 = m_b/m_t$ is fixed in the LET model. Likewise, the mixing angle α^{2HDM} of the CP-even scalars in the 2HDM can be taken to be a free parameter: the $\lambda_i^{\mathrm{2HDM}}$ are usually rewritten in terms of the scalar masses and α^{2HDM}. However, the three mixing angles of the CP-even scalars in the SB model cannot be treated as free parameters: they are approximately fixed by the value of β_1 unless at least one of the new scalars becomes light.

B. LET-model scalar spectrum

Now let us consider the scalar sector of the LET model. Compared to the SB model, it contains an additional bidoublet Φ_2 with eight real scalar components. This makes 14 physical scalars in total: five CP-even states h^0, H_1^0, H_2^0, H_3^0, H_4^0; three CP-odd states A_1^0, A_2^0, A_3^0; and three pairs of charged states $H_1^\pm$, $H_2^\pm$, $H_3^\pm$. Their definitions and masses are given in Sec. B. The CP-even states h^0, H_1^0 have masses of order v, whereas H_2^0, H_3^0, H_4^0 have masses of order M. This is not surprising: if we decouple the bidoublet Φ_2 from the model, we get one light state h^0 and two heavy states. Since Φ_1 and Φ_2 are copies of the same representation, we expect that Φ_2 adds one light and one heavy scalar to the spectrum as well. The CP-odd state A_1^0 is light, whereas A_2^0, A_3^0 are heavy. Again, this is not surprising. In the SB model, the CP-odd components of the bidoublet Φ_1 give rise to one Goldstone and one heavy state. Thus we would expect Φ_2 to contribute one heavy state as well. Since there are no more would-be Goldstones, the other CP-odd component of Φ_2 becomes a massive state with a mass of order v. Similarly, $H_1^\pm$ is light whereas $H_2^\pm$, $H_3^\pm$ have masses of order M.

IV. TRINIFICATION PHENOMENOLOGY

A. The SB model

Now we turn to the phenomenological scenarios that are allowed by the scalar sector of the trinification model. As a first step towards understanding the trinification phenomenology, we consider the phenomenological scenarios that are possible in the SB model. The free parameter space of the SB model is spanned by M and the five scalar parameters λ_i. A full analysis of this parameter space and the possible signatures is beyond the scope of this work. Instead, we define a set of benchmark points that lead to distinct phenomenological features. To get a feel for the possibilities, consider the scalar masses given in Eq. (B2). The mass of h^0 can be adjusted by changing the values of λ_1, λ_2, λ_3, λ_4. We tune these parameters such that $m_{h^0} = 126$ GeV for each benchmark. The leading contributions to $m_{H_1^0}$, m_{A^0}, $m_{H^\pm}$ are all given by $\sqrt{\lambda_5}M$, so we expect them to have similar masses, with $\mathcal{O}(v)$ mass splittings. On the other hand, $m_{H_2^0}$ is proportional to $\sqrt{\lambda_3}M$, which can be tuned independently of the other scalar masses. Thus we expect the SB model to allow for different mass hierarchies or compressed spectra, depending on the magnitudes of λ_3, λ_5.

If any of the parameters λ_3, λ_5 have $\mathcal{O}(\xi^2)$ values, some of the new scalars may obtain $\mathcal{O}(v)$ masses. Thus a number of phenomenologically different scenarios are possible. If λ_3, λ_5 are not too small, all new scalars obtain $\mathcal{O}(M)$ masses, beyond experimental reach. We denote these benchmarks as having a single large hierarchy (SLH); an additional hierarchy between H_1^0, A^0, $H^\pm$ on one side and H_2^0 on the other side is possible, but of little phenomenological interest. For $\lambda_5 \sim \mathcal{O}(\xi^2)$ but not too small λ_3, the 2HDM-like scalars H_1^0, A^0, $H^\pm$ all have $\mathcal{O}(v)$ masses and could be observed at the LHC. We choose two parameter sets such that these particles have masses in the $\mathcal{O}(100\ \mathrm{GeV})$ ballpark, and denote these benchmarks as

2HDM-1 and 2HDM-2 since they have a 2HDM-like spectrum at low energies. For $\lambda_3 \sim \mathcal{O}(\xi^2)$ but sizable λ_5, the fermiophobic state H_2^0 lies within experimental reach [33]. We choose two parameter sets such that $m_{H_2^0}$ lies in the $\mathcal{O}(100\ \text{GeV})$ range and denote these benchmarks as light fermiophobic (LF). Note that for small λ_3, the parameters λ_4, λ_5 need to be chosen sufficiently small to ensure that $m_{h^0}^2$ remains positive [see Eq. (B2)]. This means that the 2HDM-like scalars have masses well below M. A combination of the 2HDM-like and LF scenarios is possible as well: if both λ_3 and λ_5 are sufficiently small, all new scalars could have masses within experimental reach. Again, we choose two parameter sets and refer to these benchmarks as Compressed for having a spectrum compressed around the electroweak scale.

We also consider two special cases of the LF scenario. For small enough λ_3, H_2^0 can have a mass in the $\mathcal{O}(1\ \text{GeV})$ ballpark. Such a state would decay into pairs of photons only, since H_2^0 is fermiophobic. If the signal strength for its decay is low enough, it could have escaped detection so far; we discuss the relevant experimental constraints in more detail in Sec. VI. We refer to this scenario as having a very light fermiophobic (VLF) Higgs. The second special case is when h^0 and H_2^0 are approximately degenerate. If their mass difference is less than their widths, both states would contribute to the signal strength used for the Higgs discovery, leading to a "twin Higgs" [34–36]. This might result in deviations of the measured Higgs couplings from their Standard Model values. We tweak the parameters such that $m_{h^0,H_2^0} = 126\ \text{GeV}$ and denote the corresponding benchmarks as Twin-1 and Twin-2.

For each benchmark point, we use the values $v = 246\ \text{GeV}$, $\beta_1 = 0.0166$ as well as the experimental values $\sin^2\theta_W = 0.23126$, $g_L = 0.65170$, and our best fit $\theta'_W = 0.62$ as in Sec. A. The other gauge couplings are fixed by the identities $g_R = g_L \tan\theta_W / \sin\theta'_W$, $2g' = g_L \tan\theta_W / \cos\theta'_W$. As for the scale M, we consider both a high scale $M = 10^{10}$ GeV well outside experimental reach and a lower scale $M = 10^4$ GeV just beyond LHC reach. We ensure that the constraints for vacuum stability and S-matrix unitarity are satisfied. Multi-Higgs potentials in general can have several minima. Determining the global minimum of the potential is already challenging in the 2HDM [37]. We could not check that our minimum is the global one. The corresponding parameter values are given in Table I. Note that except for the SLH scenario, all benchmarks contain very small values for λ_3, λ_4 and/or λ_5: these parameters need to have $\mathcal{O}(v^2/M^2)$ values to compensate for the large VEV of the corresponding scalar invariants. This makes these scenarios unnatural.

To calculate the scalar masses we do not use the approximations in Eq. (B2), since subleading terms in ξ may become large for small λ_3 and/or λ_5. Instead, we evaluate the mass matrix numerically in MATHEMATICA [38] and then extract the masses and mass eigenstates. The corresponding particle masses are given in Table II. The scalar mass eigenstates are almost equal to the gauge eigenstates in most benchmarks: mixings are mostly below the percent level. In the Compressed-2 benchmark, there is a 2% mixing of $h_{1,11}^0$ with h_R^0. Only Twin-2 gives large scalar mixing: in terms of squares of amplitudes, the SM-like Higgs h^0 is 62% $h_{1,11}^0$ and 38% h_R^0, whereas the fermiophobic Higgs H_2^0 is 38% $h_{1,11}^0$ and 62% h_R^0; mixing with $h_{1,22}^0$ is negligible.

B. The LET model

In the SB model, the new physics decouples from the SM unless some of the dimensionless scalar parameters are set

TABLE I. Definitions of the benchmark points for the SB model in terms of the free parameters M (in GeV) and λ_i. The parameter values $v = 246$ GeV, $\beta_1 = 0.0166$, $\sin^2\theta_W = 0.23126$, $g_L = 0.65170$, $\theta'_W = 0.62$, $g_R = g_L \tan\theta_W / \sin\theta'_W$, $2g' = g_L \tan\theta_W / \cos\theta'_W$ are kept fixed.

Benchmark	M	λ_1	λ_2	λ_3	λ_4	λ_5
SLH-1	10^{10}	0.24	0.24	0.47	0.32	0.2
SLH-2	10^4	0.24	0.24	0.47	0.32	0.2
2HDM-1	10^{10}	0.41	0.4	0.44	0.49	5×10^{-15}
2HDM-2	10^4	0.41	0.4	0.44	0.49	5×10^{-3}
LF-1	10^{10}	0.133	0.13	2×10^{-15}	1×10^{-12}	3×10^{-7}
LF-2	10^4	0.14	0.14	2×10^{-3}	5.5×10^{-3}	0.6
Compressed-1	10^{10}	0.133	0.13	1.1×10^{-15}	1×10^{-12}	5×10^{-15}
Compressed-2	10^4	0.15	0.14	1.1×10^{-3}	5.2×10^{-3}	5×10^{-3}
VLF-1	10^{10}	0.133	0.13	1×10^{-20}	1×10^{-14}	2×10^{-8}
VLF-2	10^4	0.13	0.13	4.5×10^{-7}	4×10^{-5}	0.7
Twin-1	10^{10}	0.13	0.133	1.58×10^{-16}	1×10^{-16}	1×10^{-10}
Twin-2	10^4	0.131	0.131	1.59×10^{-4}	1×10^{-5}	0.1

TABLE II. Scalar masses for the benchmark points defined in Table I. All masses are given in GeV. The mass of the SM-like Higgs h^0 has been tuned to 126 GeV in each case.

Benchmark point	$m_{H_1^0}$	m_{A^0}	$m_{H^\pm}$	$m_{H_2^0}$
SLH-1	3.2×10^9	3.2×10^9	3.2×10^9	6.9×10^9
SLH-2	3.2×10^3	3.2×10^3	3.2×10^3	6.9×10^3
2HDM-1	488	488	500	6.6×10^9
2HDM-2	488	488	500	6.6×10^3
LF-1	3.9×10^6	3.9×10^6	3.9×10^6	447
LF-2	5.5×10^3	5.5×10^3	5.5×10^3	448
Compressed-1	496	496	500	332
Compressed-2	496	496	500	334
VLF-1	1.0×10^6	1.0×10^6	1.0×10^6	1.0
VLF-2	5.9×10^3	5.9×10^3	5.9×10^3	0.9
Twin-1	7.1×10^4	7.1×10^4	7.1×10^4	126
Twin-2	2.2×10^3	2.2×10^3	2.2×10^3	126

to $\mathcal{O}(\xi^2)$ values. The reason is the fact that there is a large hierarchy $v \ll M$ among the VEV parameters of Φ_1, Φ_R. The picture changes with the inclusion of the bidoublet Φ_2, since its VEV parameters are bounded by the electroweak scale. In the absence of a large hierarchy between the VEV components of Φ_1 and Φ_2, we expect that the LET model allows for large mixing between the components of both bidoublets if the dimensionless scalar-potential parameters have $\mathcal{O}(1)$ values. Hence, the model naturally contains new scalar particles with $\mathcal{O}(v)$ masses. As in the SB model, significant mixing of Φ_1, Φ_2 with the components of Φ_R is only expected for unnaturally small values of some of the parameters.

These insights have important consequences for the benchmark scenarios considered in the previous section. The SLH scenarios have no analogon in the LET model: there is always new physics within experimental reach. The 2HDM-like, LF, VLF and Twin scenarios become natural possibilities, since the 2HDM-like scalars can naturally have $\mathcal{O}(v)$ masses. Moreover, mixing of Φ_1 and Φ_2 may make these scalars fermiophobic, in which case this scenario could be distinguished from the usual 2HDM. Hence, we expect the LET model to be predictive: it allows for phenomenologically interesting, experimentally testable scenarios, since the new physics does not decouple from the SM in the large-M limit.

In the following, we discuss the prospects for measuring the Higgs-coupling modifications in the context of the LET model. To this end, we define a new set of benchmark points, inspired by the considerations given above. As a starting point for choosing the parameter values, we observe the following about the scalar masses in Eq. (B3). The main contribution to m_{h^0} is given by $\lambda_1 + \lambda_2 c_{\beta_1}^2$, with an overall scaling factor c_α^2 due to the presence of the second bidoublet. This means that a smaller α is generally accompanied by a smaller value for $\lambda_1 + \lambda_2 c_{\beta_1}^2$. Similarly, $m_{H_1^0}$ is mainly determined by $\tilde{\lambda}_1 + \tilde{\lambda}_2 c_{\beta_2}^2$ with an overall factor s_α^2, so smaller values of α should be compensated by larger values of $\tilde{\lambda}_1 + \tilde{\lambda}_2 c_{\beta_2}^2$. The $h^0 - H_1^0$ mass difference and mixing are governed by $s_{(2\alpha)}$ as well as the scalar parameters $\tilde{\lambda}_{5,6,7,8,9,10}$, so we tune these parameters until we have a parameter set that corresponds to the desired benchmark scenario. The scalar H_4^0 has $m_{H_4^0} \approx \sqrt{\lambda_3} M$, so we should take $\lambda_3 > 0$. The squared masses of A_1^0, $H_1^\pm$ are determined by $\tilde{\lambda}_{6,7,9,10}$ with an overall minus sign, so we take these parameters to be negative to guarantee a positive-definite mass matrix. Positivity of the squared masses of H_2^0, A_2^0, $H_2^\pm$ requires $\lambda_5 > 0$, and the squared masses of H_3^0, A_3^0, $H_3^\pm$ require $\tilde{\lambda}_4 / c_{(2\beta_2)} > 0$. We tune the parameters such that $m_{h^0} = 126$ GeV is fixed and enforce a set of vacuum stability conditions. The parameter values for the benchmark points are given in Table III, and the resulting scalar masses are given in Table IV.

We have defined two 2HDM-like benchmarks, in which the scalars H_1^0, A_1^0, $H_1^\pm$ all have masses in the $\mathcal{O}(100$ GeV) range. In 2HDM-3, the state h^0 is almost purely $h_{1,11}^0$, whereas H_1^0 is 97% $h_{2,11}^0$ and 3% $h_{2,22}^0$. The state A_1^0 ($H_1^\pm$) is 87% $a_{1,11}^0$ ($h_{1,21}^\pm$) and 13% $a_{2,11}^0$ ($h_{2,21}^\pm$). The mixings are even larger in the 2HDM-4 benchmark: h^0 is 74% $h_{1,11}^0$, 15% $h_{2,11}^0$, and 11% $h_{2,22}^0$ whereas H_1^0 is 25% $h_{1,11}^0$, 43% $h_{2,11}^0$ and 32% $h_{2,22}^0$. The state A_1^0 ($H_1^\pm$) is 18% $a_{1,11}^0$ ($h_{1,21}^\pm$),

TABLE III. Benchmark-point definitions for the LET model. The values $v = 246$ GeV, $M = 10^{10}$ GeV, $\beta_1 = 0.0166$ are kept fixed.

	2HDM-3	2HDM-4	VLF-3	Twin-3	Twin-4
$\sin\alpha$	0.93	0.43	0.50	0.72	0.33
$\sin\beta_2$	0.17	0.65	0.17	0.16	0.11
λ_1	1.0	0.20	0.13	0.34	0.17
λ_2	1.0	0.18	0.13	0.35	0.16
λ_3	0.50	0.50	0.50	0.50	0.42
λ_4	0.010	0.12	0.13	0.27	0.12
λ_5	0.20	0.50	0.20	0.20	0.50
$\tilde{\lambda}_1$	0.40	1.3	0.27	0.34	1.3
$\tilde{\lambda}_2$	0.40	1.3	0.27	0.34	1.2
$\tilde{\lambda}_3$	0.27	0.20	0.27	0.27	0.19
$\tilde{\lambda}_4$	0.20	0.10	0.20	0.20	1.0
$\tilde{\lambda}_5$	0.20	0.046	0.54	0.32	0.060
$\tilde{\lambda}_6$	−0.40	−0.50	−0.43	−0.42	−0.30
$\tilde{\lambda}_7$	−0.24	−0.20	−0.24	−0.24	−0.30
$\tilde{\lambda}_8$	0.84	0.95	0.83	0.84	1.0
$\tilde{\lambda}_9$	−0.050	−0.10	−0.04	−0.053	−0.10
$\tilde{\lambda}_{10}$	−0.30	−0.30	−0.30	−0.30	−0.30

TABLE IV. Scalar masses for each of the benchmark points defined in Table III. All masses are in GeV.

	2HDM-3	2HDM-4	VLF-3	Twin-3	Twin-4
m_{h^0}	126	126	126	126	126
$m_{H_1^0}$	182	148	3.9	126	126
$m_{H_2^0}$	3.2×10^9	5.0×10^9	3.2×10^9	3.2×10^9	5.0×10^9
$m_{H_3^0}$	3.3×10^9	5.8×10^9	3.3×10^9	3.2×10^9	7.2×10^9
$m_{H_4^0}$	7.1×10^9	7.1×10^9	7.1×10^9	7.1×10^9	6.5×10^9
$m_{A_1^0}$	179	134	179	179	190
$m_{A_2^0}$	3.2×10^9	5.0×10^9	3.2×10^9	3.2×10^9	5.0×10^9
$m_{A_3^0}$	3.3×10^9	5.8×10^9	3.3×10^9	3.2×10^9	7.2×10^9
$m_{H_1^\pm}$	171	135	173	173	173
$m_{H_2^\pm}$	3.2×10^9	5.0×10^9	3.2×10^9	3.2×10^9	5.0×10^9
$m_{H_3^\pm}$	3.3×10^9	5.8×10^9	3.3×10^9	3.2×10^9	7.2×10^9

47% $a^0_{2,11}$ ($h^\pm_{2,21}$), and 35% $a^0_{2,22}$ ($h^\pm_{2,12}$). In both cases, the 2HDM-like scalars have suppressed couplings to fermions with respect to the type-II 2HDM.

We also define the VLF-3 scenario, in which H_1^0 has a mass of only a few GeV. The states A_1^0, $H_1^\pm$ have masses within experimental reach. The scalar mixing is significant: h^0 is 65% $h^0_{1,11}$, 34% $h^0_{2,11}$, and 1% $h^0_{2,22}$, so we expect reduced fermion couplings. The state H_1^0 is 35% $h^0_{1,11}$, 63% $h^0_{2,11}$, and 2% $h^0_{2,22}$. Since it is light and mainly fermiophobic, it could have evaded the LEP searches. The state A_1^0 ($H_1^\pm$) is 25% $a^0_{1,11}$ ($h^\pm_{1,21}$), 73% $a^0_{2,11}$ ($h^\pm_{2,21}$), and 2% $a^0_{2,22}$ ($h^\pm_{2,12}$).

Furthermore, we define two Twin benchmarks with different amounts of scalar mixing. For Twin-3, the state h^0 is 87% $h^0_{1,11}$ and 13% $h^0_{2,11}$, whereas H_1^0 is 13% $h^0_{1,11}$, 85% $h^0_{2,11}$, and 2% $h^0_{2,22}$. The lightest CP-odd and charged states are almost 50-50 mixtures of fermiophilic and fermiophobic states: A_1^0 ($H_1^\pm$) is 51% $a^0_{1,11}$ ($h^\pm_{1,21}$), 47% $a^0_{2,11}$ ($h^\pm_{2,21}$), and 1% $a^0_{2,22}$ ($h^\pm_{2,12}$). For Twin-4, h^0 is almost purely $h^0_{1,11}$, whereas H_1^0 is 99% $h^0_{2,11}$ and 1% $h^0_{2,22}$. The lightest CP-odd and charged states are mostly fermiophobic: A_1^0 ($H_1^\pm$) is 11% $a^0_{1,11}$ ($h^\pm_{1,21}$), 88% $a^0_{2,11}$ ($h^\pm_{2,21}$), and 1% $a^0_{2,22}$ ($h^\pm_{2,12}$).

V. HIGGS-COUPLING MODIFICATIONS

In the SM, the Higgs couplings are fixed in terms of the particle masses and the VEV of the Higgs field. Hence, an independent measurement of these couplings provides an important test of the SM. These couplings are generally modified in the presence of an extended Higgs sector [39]. The Higgs-coupling modifications Δ_x are defined as the deviations of the Higgs couplings $g_x \equiv g_{h^0xx}$ from their SM values, where x is any SM particle and g_{h^0xx} is the coefficient of the operator h^0xx in the Lagrangian:

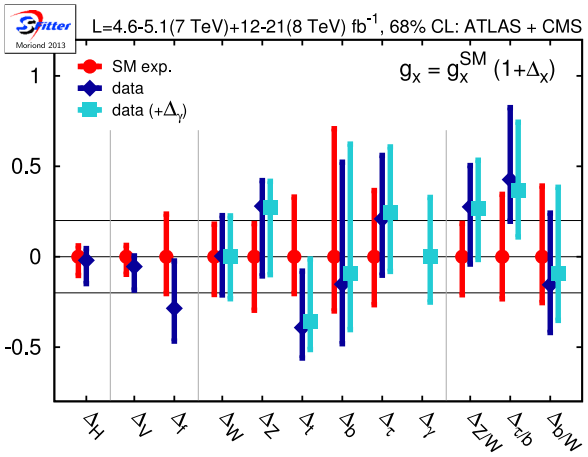

FIG. 1 (color online). Most recent fit of the Higgs-coupling modifications to LHC data. The red points correspond to the expected SM result $\Delta_x = 0$, whereas the dark blue points give the results from the data if the photon coupling is assumed to be determined by the W and t loops only. The light blue points give the results if a free coupling shift in Δ_γ due to new physics is allowed. Figure taken from Ref. [39].

$$g_x = (1 + \Delta_x) g_x^{\mathrm{SM}}. \tag{12}$$

The loop-induced Higgs coupling to photons can be written as follows:

$$g_\gamma = (1 + \Delta_\gamma^{\mathrm{SM}} + \Delta_\gamma) g_\gamma^{\mathrm{SM}}. \tag{13}$$

Here $\Delta_\gamma^{\mathrm{SM}}$ is the coupling modification that is induced by coupling modifications of the Standard Model particles generating the coupling. The term Δ_γ represents contributions from non-SM particles running in the loops. The Higgs-coupling modifications have been extracted from LHC data using the tool SFitter [39–42] (see Fig. 1).

A. The SB model

The Higgs-coupling modifications of the SB model are given in Sec. C. In order to see whether our benchmark scenarios could be distinguished from the SM in experiment, we calculate the Higgs-coupling modifications numerically for each benchmark point. The results are listed in Table V.

For the SLH benchmarks, the modification of the quartic Higgs self-coupling is as large as 83%, whereas the other couplings have negligible deviations from their SM values. Hence, if we could measure both Higgs self-couplings, a SB model with a large hierarchy could be distinguished from the SM by the strength of the quartic Higgs self-coupling, even if M is large. Like in the 2HDM [43], the self-couplings are generally modified due to the more complicated structure of the scalar potential, although these modifications may also vanish along some directions of the parameter space (see Sec. C).

TABLE V. Numerical results for the Higgs-coupling modifications for the benchmark points defined in Table I.

Benchmark point	Δ_W	Δ_Z	Δ_t	Δ_b	Δ_γ	$\Delta_{\lambda_{3h}}$	$\Delta_{\lambda_{4h}}$
SLH-1	-1.4×10^{-16}	0.0	-1.4×10^{-16}	0.0	-5.0×10^{-17}	0.0	0.83
SLH-2	-1.4×10^{-4}	-4.1×10^{-4}	-1.4×10^{-4}	2.1×10^{-3}	-5.0×10^{-5}	-4.2×10^{-4}	0.83
2HDM-1	-1.6×10^{-6}	-1.6×10^{-6}	-3.2×10^{-5}	0.11	-1.7×10^{-3}	-9.7×10^{-5}	2.1
2HDM-2	-3.8×10^{-4}	-6.4×10^{-4}	-4.1×10^{-4}	0.11	-1.6×10^{-3}	-1.2×10^{-3}	2.1
LF-1	-6.2×10^{-7}	-6.2×10^{-7}	-6.2×10^{-7}	-6.2×10^{-7}	-2.6×10^{-11}	-1.9×10^{-6}	1.2×10^{-5}
LF-2	-2.9×10^{-3}	-3.1×10^{-3}	-2.9×10^{-3}	1.1×10^{-3}	5.1×10^{-5}	-8.6×10^{-3}	5.5×10^{-2}
Compressed-1	-1.6×10^{-7}	-1.6×10^{-7}	-9.6×10^{-6}	3.4×10^{-2}	-1.6×10^{-3}	-9.6×10^{-6}	-1.4×10^{-5}
Compressed-2	-9.1×10^{-3}	-9.4×10^{-3}	-9.1×10^{-3}	3.5×10^{-2}	-1.5×10^{-3}	-2.7×10^{-2}	7.1×10^{-2}
VLF-1	-3.6×10^{-7}	-3.6×10^{-7}	-3.6×10^{-7}	-3.6×10^{-7}	-4.1×10^{-10}	-1.1×10^{-6}	-2.2×10^{-6}
VLF-2	-6.6×10^{-4}	-9.3×10^{-4}	-6.6×10^{-4}	-2.2×10^{-3}	-8.8×10^{-5}	-2.0×10^{-3}	-4.0×10^{-3}
Twin-1	-1.9×10^{-7}	-1.9×10^{-7}	-1.9×10^{-7}	1.4×10^{-6}	-8.1×10^{-8}	-5.6×10^{-7}	-7.5×10^{-7}
Twin-2	−0.21	−0.21	−0.21	−0.18	6.9×10^{-4}	−0.52	−0.61

For the 2HDM-like benchmarks, there is an 11% increase of the Higgs coupling to b quarks. The reason is that the main contribution to Δ_b in this scenario is proportional to $\xi^2/\lambda_5 \sim 0.1$. The W, Z and t couplings obtain similar modifications, but these are suppressed by factors $s^2_{(4\beta_1)} \sim 10^{-3}$ and $s^2_{\beta_1} \sim 10^{-4}$, respectively. Hence, the 2HDM-like hierarchy is characterized by an increase in only the b coupling. The quartic Higgs self-coupling is enhanced by a factor 3.

The LF, Compressed, and VLF benchmarks have coupling modifications at or below the percent level. These scenarios would not be distinguishable from the SM via the Higgs-coupling modifications. The Twin-1 benchmark has very small coupling modifications as well, but the Twin-2 benchmark shows 20% reductions of all tree-level Higgs couplings and 50%–60% decreases of both self-couplings. Currently, the errors on the Higgs couplings are still large enough to allow a 20% deviation (see Fig. 1). If the errors can be reduced after the 14 TeV run, the Twin-2 benchmark can be put to the test.

B. The LET model

Because of the large number of free parameters and scalar mixing angles, we restrict ourselves to a numerical analysis of the Higgs-coupling modifications for the benchmark points defined in Sec. IV B. The resulting coupling modifications have been summarized in table VI. Note that contrary to the SB model, the photon-coupling modification is not negligibly small any more: the charged scalar $H_1^\pm$ has a mass of order v and, hence, yields a sizable contribution to the effective photon coupling.

The 2HDM-3 benchmark has large coupling modifications: the couplings to $V = W, Z$ are suppressed by a factor 0.3, whereas the couplings to t, b are enhanced by almost a factor 3. This is not surprising: the W, Z couplings of the SB model are proportional to v, whereas the t, b couplings are proportional to $m_{t,b}/v$. In the LET model, we have to substitute $v \to v\cos\alpha$ [see Eq. (7)]. Since h^0 is almost purely $h^0_{1,11}$ in the 2HDM-3 benchmark, the W, Z couplings are suppressed by $\cos\alpha = 0.36$ whereas the t, b couplings are enhanced by $1/\cos\alpha = 2.8$. This benchmark point is clearly incompatible with the measured coupling modifications in Fig. 1. In contrast, the 2HDM-4 benchmark has smaller but still sizable coupling modifications. The V couplings are suppressed by $\cos\alpha = 0.90$, but the total coupling is a few percent higher because of the contribution from the second bidoublet. On the other hand, the quark couplings are enhanced by a factor $1/\cos\alpha = 1.11$, but the total coupling modifications are negative: since h^0 contains a significant admixture of the fermiophobic Φ_2, the t, b couplings are reduced. The coupling modifications for 2HDM-4 are consistent with the measured coupling modifications.

The VLF-3 scenario has large mixing between the fermiophilic and fermiophobic scalar gauge eigenstates. As such, there is again a tension between $\cos\alpha$ and $\Phi_1 - \Phi_2$ mixing. The resulting coupling modifications are at the percent level, all compatible with the measured values.

Like the 2HDM-3 benchmark, the Twin-3 scenario has large coupling modifications. The W, Z couplings are reduced by about 60%, mostly due to interference between the contributions of the fermiophobic and fermiophilic

TABLE VI. Higgs-coupling modifications for the benchmark points of the LET model, defined in Table III.

	2HDM-3	2HDM-4	VLF-3	Twin-3	Twin-4
Δ_W	−0.69	−0.01	−0.01	−0.61	−0.06
Δ_Z	−0.69	−0.001	−0.001	−0.60	−0.05
Δ_t	1.8	−0.05	−0.07	0.34	0.06
Δ_b	1.8	−0.05	−0.07	0.34	0.06
Δ_γ	−0.05	−0.09	−0.07	−0.03	−0.05

scalar components. The t, b couplings are enhanced by 34%: the factor $1/\cos\alpha = 1.4$ is slightly reduced by $\Phi_1 - \Phi_2$ mixing. This benchmark point is incompatible with the data. However, the Twin-4 scenario has percent-level coupling modifications, compatible with the measured values. This is because the V couplings are suppressed by $\cos\alpha = 0.94$ and the fermion couplings are enhanced by $1/\cos\alpha = 1.06$, and $\Phi_1 - \Phi_2$ mixing is negligible.

We have illustrated that the LET model is predictive and allows for various interesting phenomenological scenarios. The model allows for large coupling modifications as well as moderate ones that can be expected to be measurable; hence, the model is testable. A more thorough analysis of the parameter space is required to see which parameter values are preferred by experiment.

VI. VERY LIGHT FERMIOPHOBIC SCALARS

The VLF scenario contains a fermiophobic scalar particle with a mass of $\mathcal{O}(1\ \text{GeV})$ in addition to the SM-like Higgs. Such a particle would only decay into pairs of photons, and is not necessarily ruled out since it could have escaped detection so far. We now review the experimental bounds that are relevant to this scenario.

Fermiophobic Higgs particles are not unique to the SB model: they also appear in a type-I 2HDM with $\alpha = \pi/2$ [44] and in models with $SU(2)_L$-triplet Higgs fields [45,46]. Mass bounds from direct searches are readily available in the literature [47]. Assuming SM cross sections, the four LEP experiments [48–51] have placed a lower limit $m_H > 107$ GeV on the mass of a fermiophobic Higgs by looking for decays into pairs of photons. More recent searches by ATLAS [52] and CMS [53] in the diphoton channel as well as the WW, ZZ channels [54] extend this lower limit to $m_H > 194$ GeV. However, the cuts on the energy of the photon pair in the LEP analyses make these searches insensitive to fermiophobic Higgs particles with masses below 10 GeV.

In order to see to what extent the lower mass bound applies to the fermiophobic Higgs H_2^0 of the SB model, we need to examine its couplings to SM particles. The field Φ_R has no tree-level couplings to fermions, and its neutral component is a SM singlet. Hence, H_2^0 only couples to the SM through $W - W'$ mixing, $Z - Z'$ mixing and scalar mixing. The former two are negligible since they are of order ξ^2. Scalar mixing can become substantial in the Twin scenario, but it is negligible in the VLF scenario. Hence, H_2^0 has only $\mathcal{O}(\xi^2)$ couplings to the SM in the SB model, and, therefore, the experimental bounds are evaded trivially.

This may change in the LET model. We have seen that a very light fermiophobic Higgs with a mass of a few GeV becomes a natural possibility. Since it is Φ_2-like, it has significant couplings to W, Z, distinguishing it from the very light fermiophobic Higgs of the SB model. Hence, such a state could have significant production rates at the LHC. A more thorough analysis of the production cross section is necessary in order to predict the signal strength, which is beyond the scope of this work.

VII. A TWIN HIGGS SCENARIO

The Higgs signal strength in each channel has been measured at the LHC [2,55,56]. These measurements constrain the Twin scenario. In order to compare the Twin benchmarks to these experimental results, we have to consider the production cross sections and branching ratios for both h^0 and H_2^0.

We parametrize the twin states $S^0 = h^0, H_2^0$ in terms of the gauge eigenstates as

$$\begin{aligned} h^0 &= a_1 h^0_{1,11} + a_2 h^0_{1,22} + a_3 h^0_R, \\ H_2^0 &= a_1^{\text{FP}} h^0_{1,11} + a_2^{\text{FP}} h^0_{1,22} + a_3^{\text{FP}} h^0_R, \end{aligned} \tag{14}$$

where FP stands for fermiophobic. The coefficients for the Twin-1 benchmark are given by

$$\begin{aligned} (a_1, a_2, a_3) &= (0.9999, 0.0166, 0.0006), \qquad \text{(Twin-1)} \\ (a_1^{\text{FP}}, a_2^{\text{FP}}, a_3^{\text{FP}}) &= (-0.0006, -0.00001, 0.9999), \end{aligned} \tag{15}$$

whereas for the Twin-2 benchmark they are

$$\begin{aligned} (a_1, a_2, a_3) &= (0.7874, 0.0136, -0.6162), \qquad \text{(Twin-2)} \\ (a_1^{\text{FP}}, a_2^{\text{FP}}, a_3^{\text{FP}}) &= (0.6162, 0.0096, 0.7876). \end{aligned} \tag{16}$$

We need to find the signal strengths $\mu_x(S^0)$ for each decay channel $S^0 \to xx$:

$$\mu_x(S^0) = \frac{\sigma(pp \to S^0) \times BR(S^0 \to xx)}{\sigma(pp \to h^0)_{\text{SM}} \times BR(h^0 \to xx)_{\text{SM}}}, \tag{17}$$

where $\sigma(pp \to S^0)$ is the production cross section for S^0. Then we need to add the signal strengths of h^0 and H_2^0. In order to estimate the magnitude of the deviations from their SM values, we neglect loop corrections in the following discussion.

At the LHC, the Higgs can be produced in vector-boson fusion, VH associated production, gluon fusion, and production in association with $t\bar{t}$ pairs [57]. The former two processes are proportional to the Higgs coupling to vector bosons, whereas the latter two scale with the top coupling (the main contribution to gluon fusion comes from a top-quark loop). For h^0, we have $\Delta_1 \equiv \Delta_W = \Delta_Z = \Delta_t = a_1 - 1$ (see Sec. C, we neglect $\mathcal{O}(\xi^2)$ and $\mathcal{O}(\beta_1)$ corrections). Hence, as a tree-level approximation we have

$$\frac{\sigma(pp \to h^0)}{\sigma(pp \to h^0)_{\text{SM}}} = a_1^2. \tag{18}$$

Similarly, $\Delta_1^{\rm FP} \equiv \Delta_W^{\rm FP} = \Delta_Z^{\rm FP} = \Delta_t^{\rm FP} = a_1^{\rm FP} - 1$, up to $\mathcal{O}(\xi^2)$ and $\mathcal{O}(\beta_1)$ corrections. Hence, at tree level we have

$$\frac{\sigma(pp \to H_2^0)}{\sigma(pp \to h^0)_{\rm SM}} = (a_1^{\rm FP})^2. \tag{19}$$

For the Twin-1 benchmark we have $a_1^2 = 1$, $(a_1^{\rm FP})^2 = 4 \times 10^{-7}$ [see Eq. (15)]. That is, h^0 is produced at the same rate as the SM Higgs, whereas H_2^0 production is suppressed. In the Twin-2 benchmark, however, both states have a significant production rate since $a_1^2 = 0.62$, $(a_1^{\rm FP})^2 = 0.38$.

As for the branching ratios, we only take into account the decay channels listed in Table VII; all other channels have negligibly small branching ratios. The given SM values were calculated with HDecay [58] using $m_h = 126$ GeV. We estimate the corresponding branching ratios of the SB model using the Higgs-coupling modifications. According to Eq. (10) the b quark and the τ couple to the same scalar gauge eigenstate, namely $h^0_{1,22}$. We thus assume that $\Delta_\tau = \Delta_b \equiv \Delta_2$ and $\Delta_\tau^{\rm FP} = \Delta_b^{\rm FP} \equiv \Delta_2^{\rm FP}$.

Now we are ready to calculate the branching ratios of the SB model. The partial decay widths for the h^0 and H_2^0 decays into $y_1y_1 = WW$, ZZ, gg, $\gamma\gamma$, cc scale with, respectively, $(1+\Delta_1)^2$ and $(1+\Delta_1^{\rm FP})^2$, whereas they scale with, respectively, $(1+\Delta_2)^2$ and $(1+\Delta_2^{\rm FP})^2$ for the $y_2y_2 = bb$, $\tau\tau$ decay channels. Thus the branching ratios for the SB model are given by

$$\begin{aligned}
BR(h^0 \to xx) &= \frac{(1+\Delta_x)^2 BR(h^0 \to xx)_{\rm SM}}{(1+\Delta_1)^2 \widetilde{BR}_1 + (1+\Delta_2)^2 \widetilde{BR}_2}, \\
BR(H_2^0 \to xx) &= \frac{(1+\Delta_x^{\rm FP})^2 BR(h^0 \to xx)_{\rm SM}}{(1+\Delta_1^{\rm FP})^2 \widetilde{BR}_1 + (1+\Delta_2^{\rm FP})^2 \widetilde{BR}_2}, \\
\widetilde{BR}_1 &\equiv \sum_{y_1 = W,Z,g,\gamma,c} BR(h^0 \to y_1y_1)_{\rm SM}, \\
\widetilde{BR}_2 &\equiv \sum_{y_2 = b,\tau} BR(h^0 \to y_2y_2)_{\rm SM}.
\end{aligned} \tag{20}$$

TABLE VII. Branching ratios and signal strengths of h^0 and H_2^0 decays in the Twin-2 benchmark of the SB model. The SM values of the branching ratios were calculated with HDecay [58] for $m_h = 126$ GeV. We neglect the branching ratios for the $\mu\mu$, ss, tt, $Z\gamma$ decay channels.

	WW	ZZ	gg	$\gamma\gamma$	cc	bb	$\tau\tau$
$BR(h^0 \to xx)_{\rm SM}$	0.216	0.027	0.077	0.002	0.026	0.594	0.057
$BR(h^0 \to xx)$	0.206	0.026	0.073	0.002	0.025	0.610	0.059
$BR(H_2^0 \to xx)$	0.235	0.029	0.084	0.002	0.028	0.566	0.054
$\mu_x(h^0)$	0.59	0.59	0.59	0.59	0.59	0.64	0.64
$\mu_x(H_2^0)$	0.41	0.41	0.41	0.41	0.41	0.36	0.36
$\mu_x(h^0) + \mu_x(H_2^0)$	1.0	1.0	1.0	1.0	1.0	1.0	1.0

In the Twin-1 benchmark we have $|\Delta_{1,2}| \ll 1$ (see Table V); hence, the branching ratios for h^0 barely deviate from their SM values. The branching ratios for H_2^0 are small, since $|1 + \Delta_{1,2}^{\rm FP}| = |a_{1,2}^{\rm FP}| \ll 1$. The branching ratios for the Twin-2 benchmark are listed in Table VII.

The total signal strength is given by the sum of the contributions from h^0 and H_2^0. Combining Eqs. (18), (19), and (20), we find

$$\begin{aligned}
\mu_{x,\rm tot} = &\frac{a_1^2(1+\Delta_x)^2}{(1+\Delta_1)^2\widetilde{BR}_1 + (1+\Delta_2)^2\widetilde{BR}_2} \\
&+ \frac{(a_1^{\rm FP})^2(1+\Delta_x^{\rm FP})^2}{(1+\Delta_1^{\rm FP})^2\widetilde{BR}_1 + (1+\Delta_2^{\rm FP})^2\widetilde{BR}_2}.
\end{aligned} \tag{21}$$

We find $\mu_{x,tot} = 1$ for the Twin-1 benchmark: h^0 contributes with the SM strength whereas H_2^0, despite its identical mass, is hardly produced and cannot show itself by decays to SM final states. The signal strengths for the Twin-2 benchmark have been summarized in Table VII. In this case two states with the same mass but different decay properties are present. Still, none of the decay channels has a total signal strength that deviates significantly from 1. The reason is that the SM contributions to the signal strength are simply divided among the two scalars.

The situation may change in the LET model, in which the fermiophobic scalar H_1^0 can be the twin partner of h^0. The state H_1^0 is a mixture of components of both Φ_1 and Φ_2. Since the latter is an $SU(2)_L$-antidoublet, it couples to W, Z. After scalar mixing, these additional contributions can give the twin Higgs a total signal strength that differs from the SM prediction. Note that the Higgs-coupling modifications of the LET model are not universal (see Table VI). This means that the Higgs production cross sections do not scale trivially, as they did in the SB model. Hence, a prediction of the twin-Higgs signal strength requires a more detailed analysis of the production cross section.

VIII. CONCLUSIONS

In this work we have studied the low-energy phenomenology of the trinification model as described in Refs. [7,19–23]. It is based on the trinification group $SU(3)_C \times SU(3)_L \times SU(3)_R$. In order to simplify our study, we have integrated out the fields that obtain masses of the order of the trinification scale. This resulted in a left-right-symmetric model with two scalar bidoublets Φ_1, Φ_2 and one right-handed doublet Φ_R. While the bidoublets obtain VEVs of the order of the weak scale, the right-handed doublet has a VEV M that describes the scale at which the left-right symmetry is broken. It may be as low as a few TeV but could also be much higher. Only Φ_1 couples to fermions. We call this effective model the low-energy trinification (LET) model. As an intermediate step towards a better understanding of the LET model, we have studied

the single-bidoublet (SB) model, a simplified model in which Φ_2 has been set to zero.

Our ansatz for the Yukawa sector was based on the Yukawa Lagrangian of the trinification model. The free parameters were used to fix the masses of the top and bottom quarks, which are the most important for comparison to experimental searches. We left out a discussion of the first and second fermion generations. An improved version of the LET model containing these lighter fermions would require the introduction of new Higgs fields, mixings with heavy states, and the consideration of renormalization-group effects.

In order to showcase the possible phenomenological scenarios of our model, we have defined a set of benchmark points for both the SB model and the LET model. In the SB model, all new scalars decouple from the SM unless we tune some of the dimensionless scalar-coupling constants to $\mathcal{O}(v^2/M^2)$ values. For such small coupling constants, interesting phenomenological scenarios are possible at low energies, like a fermiophobic scalar particle with an $\mathcal{O}(1\ \mathrm{GeV})$ mass in addition to a SM-like Higgs, higher-mass states with fermiophobic components, or a degenerate state ("twin Higgs") at 126 GeV. On the other hand, the full LET model always has at least one other CP-even scalar, one CP-odd scalar, and a pair of charged scalars with masses in the $\mathcal{O}(100\ \mathrm{GeV})$ range. They appear without tuning the coupling constants to very small values. The aforementioned phenomenological scenarios, therefore, become natural possibilities.

To show to what extent these scenarios can be distinguished from the SM in experiment, we have calculated the Higgs-coupling modifications for the benchmarks. For the SB model, they are negligibly small in most cases. However, the benchmarks of the LET model lead to sizable effects on the Higgs couplings. Parts of the parameter space can already be excluded using the known limits given in the literature.

Subsequently, we have studied the scenario with a very light fermiophobic (VLF) Higgs in more detail. Such a particle decays only into pairs of photons and escapes the currently available bounds from direct searches. For the VLF Higgs of the SB model, the signal strength is very small since it has only $\mathcal{O}(v^2/M^2)$ couplings to the SM. We argued that the VLF Higgs of the LET model may have significant production rates at the LHC. We also studied the twin Higgs scenario (degenerate Higgs state) in more detail. For the SB model, we expect no significant deviations from the SM prediction even though each of the two degenerate states has different decay properties. On the other hand, the twin Higgs of the LET model may lead to significant deviations, because the bidoublet Φ_2 can introduce direct couplings of the new state to SM particles. A more detailed analysis of the production cross section appears necessary for a detailed comparison with the measured signal strengths.

We have calculated the phenomenological scenarios of the LET model at several benchmark points and found interesting consequences for the properties of the Higgs bosons. Because of the number of coupling constants in the potential a systematic investigation of all regions of the parameter space is still missing. Nevertheless, the examples given show the large variety of possibilities still not excluded by experiment. The LET model turned out to be an interesting extension of the SM. It is predictive and most properties can be tested or constrained using forthcoming LHC data.

ACKNOWLEDGMENTS

The authors would like to thank Tilman Plehn for fruitful and stimulating discussions. J. H. thanks him, in addition, for supervising his PhD thesis and acknowledges financial support by the German Research Foundation (Deutsche Forschungsgemeinschaft).

APPENDIX A: GAUGE SECTOR OF THE LET MODEL

The gauge-boson sector consists of seven fields: $W^{1,2,3}_{L,R}$ for $SU(2)_{L,R}$ and B for $U(1)_{B-L}$. The fields W^3_L, W^3_R, and B are neutral, whereas the remaining fields mix to form the charge eigenstates $W^\pm_{L,R} \equiv (W^1_{L,R} \mp iW^2_{L,R})/\sqrt{2}$. These charged states are rotated by an angle ζ into two pairs of charged mass eigenstates $W^\pm$ and $W'^\pm$:

$$\begin{pmatrix} W^\pm \\ W'^\pm \end{pmatrix} = \begin{pmatrix} \cos\zeta & \sin\zeta \\ -\sin\zeta & \cos\zeta \end{pmatrix} \begin{pmatrix} W^\pm_L \\ W^\pm_R \end{pmatrix}. \tag{A1}$$

Here the $W^\pm$ correspond to the charged vector bosons of the SM. The $W'^\pm$ bosons are new massive vector bosons. The mixing angle is very small (we define $s_x \equiv \sin x$, $c_x \equiv \cos x$ for the sake of brevity):

$$\zeta = \frac{g_L}{g_R}\xi^2(c^2_\alpha s_{(2\beta_1)} + s^2_\alpha s_{(2\beta_2)}) + \mathcal{O}(\xi^4). \tag{A2}$$

The masses of the charged mass eigenstates are given by

$$m_W = \frac{g_L v}{2}\left(1 - \frac{\xi^2}{2}(c^2_\alpha s_{(2\beta_1)} + s^2_\alpha s_{(2\beta_2)})^2 + \mathcal{O}(\xi^4)\right),$$
$$m_{W'} = \frac{g_R M}{2}(1 + \xi^2 + \mathcal{O}(\xi^4)). \tag{A3}$$

The three neutral gauge fields mix into a massless photon A, a massive Z as in the SM, and a new massive state Z'. These states are obtained through a rotation over three mixing angles θ_W, θ'_W, η:

$$
\begin{aligned}
A &= s_{\theta_W} W_L^3 + c_{\theta_W}(s_{\theta'_W} W_R^3 + c_{\theta'_W} B),\\
Z &= c_{\theta_W} c_\eta W_L^3 + (c_{\theta'_W} s_\eta - s_{\theta_W} s_{\theta'_W} c_\eta) W_R^3\\
&\quad - (s_{\theta_W} c_{\theta'_W} c_\eta + s_{\theta'_W} s_\eta) B,\\
Z' &= -c_{\theta_W} s_\eta W_L^3 + (c_{\theta'_W} c_\eta + s_{\theta_W} s_{\theta'_W} s_\eta) W_R^3\\
&\quad + (s_{\theta_W} c_{\theta'_W} s_\eta - s_{\theta'_W} c_\eta) B. \qquad \text{(A4)}
\end{aligned}
$$

The angle θ_W is the Weinberg angle; θ'_W is an analogon of θ_W for the breaking of the left-right symmetry; and η is the $Z - Z'$ mixing angle. These angles are given in terms of the gauge couplings by

$$
\begin{aligned}
\sin\theta_W &= \frac{2g'g_R}{\sqrt{4g'^2(g_L^2+g_R^2)+g_L^2 g_R^2}},\\
\sin\theta'_W &= \frac{2g'}{\sqrt{g_R^2+4g'^2}},\\
\tan\eta &= \frac{g_R^2\sqrt{4g'^2(g_L^2+g_R^2)+g_L^2g_R^2}}{(g_R^2+4g'^2)^2}\xi^2 + \mathcal{O}(\xi^4). \qquad \text{(A5)}
\end{aligned}
$$

The masses of the states Z, Z' are given by

$$
\begin{aligned}
m_Z &= \frac{g_L v}{2\cos\theta_W}\left(1 - \frac{\xi^2\cos^4\theta'_W}{2} + \mathcal{O}(\xi^4)\right),\\
m_{Z'} &= \frac{g_R M}{2\cos\theta'_W}\left(1 + \frac{\xi^2\cos^4\theta'_W}{2} + \mathcal{O}(\xi^4)\right). \qquad \text{(A6)}
\end{aligned}
$$

The electromagnetic coupling constant is found to be

$$
e \equiv \frac{2g'g_Lg_R}{\sqrt{4g'^2(g_L^2+g_R^2)+g_L^2g_R^2}} = g_L\sin\theta_W. \qquad \text{(A7)}
$$

Constraints on the W' and Z' masses as well as their mixing angles are widely available in the literature and allow us to constrain the new parameters g_R, g', and M. Direct searches for W' and Z' have been performed in various decay channels [59], but mass bounds are only given under the assumption that the new vector bosons have the same couplings to fermions as W and Z, respectively. Hence, they do not apply to the LET model. More general constraints come from fits to electroweak precision data [60,61] and high-precision measurements [62–64]. The right-handed coupling g_R is constrained by the bound $g_R/g_L = 0.94 \pm 0.09$ from Ref. [62]. Combining this bound with Eq. (A7) and the experimental values $g_L = 0.65170 \pm 0.00008$, $e = 0.313402 \pm 0.000017$ gives a constraint on g' as well:

$$
\begin{aligned}
g_R &= 0.61 \pm 0.06,\\
g' &= 0.22 \pm 0.01. \qquad \text{(A8)}
\end{aligned}
$$

The strongest constraint on M comes from the bound $-0.00040 < \eta < 0.0026$ from Ref. [60] on the $Z - Z'$ mixing angle. Combining it with Eqs. (A5) and (A8), we find

$$
M > 3.6\ \text{TeV}. \qquad \text{(A9)}
$$

APPENDIX B: SCALAR MASS EIGENSTATES

The scalar fields Φ_j $(j = 1, 2)$, Φ_R can be parametrized in terms of gauge eigenstates as

$$
\begin{aligned}
\Phi_j &= \begin{pmatrix} \frac{v_j + h^0_{j,11} + ia^0_{j,11}}{\sqrt{2}} & h^-_{j,12} \\ h^+_{j,21} & \frac{b_j + h^0_{j,22} + ia^0_{j,22}}{\sqrt{2}} \end{pmatrix},\\
\Phi_R &= \begin{pmatrix} h^+_R & \frac{M + h^0_R + ia^0_R}{\sqrt{2}} \end{pmatrix}. \qquad \text{(B1)}
\end{aligned}
$$

After spontaneous symmetry breaking, they are mixed into eigenstates of the mass matrix.

1. Single-bidoublet model

In the SB model, only Φ_1 and Φ_R are present, containing twelve real scalar components in total. They are mixed into six Goldstone bosons and six massive particles. The scalar masses are given in terms of the model parameters by

$$
\begin{aligned}
&\frac{m^2_{h^0}}{v^2} = \lambda_1 + \lambda_2 c^2_{\beta_1} - \frac{(\lambda_4 + \lambda_5 s^2_{\beta_1})^2}{\lambda_3} + \mathcal{O}(\xi^2), \qquad \frac{m^2_{H^0_1}}{M^2} = \frac{\lambda_5}{2c_{(2\beta_1)}} - \frac{\xi^2}{2}\left(\lambda_2 c^2_{(2\beta_1)} - \frac{\lambda_5^2 s^2_{(2\beta_1)} c_{(2\beta_1)}}{\lambda_5 - 2\lambda_3 c_{(2\beta_1)}} + \mathcal{O}(\xi^2)\right),\\
&\frac{m^2_{H^0_2}}{M^2} = \lambda_3 + \xi^2\left(\frac{(\lambda_4 + \lambda_5 s^2_{\beta_1})^2}{\lambda_3} - \frac{\lambda_5^2 s^2_{(2\beta_1)} c_{(2\beta_1)}}{\lambda_5 - 2\lambda_3 c_{(2\beta_1)}} + \mathcal{O}(\xi^2)\right), \qquad \frac{m^2_{A^0}}{M^2} = \frac{\lambda_5}{2c_{(2\beta_1)}} - \frac{\lambda_2}{2}\xi^2, \qquad \frac{m^2_{H^\pm}}{M^2} = \frac{\lambda_5}{2c_{(2\beta_1)}}(1 + \xi^2 c^2_{(2\beta_1)}).
\end{aligned} \qquad \text{(B2)}
$$

Here we define h^0 as the scalar that is the most $h^0_{1,11}$-like and H^0_2 as the scalar that is the most h^0_R-like. The massive CP-odd state A^0 is a mixture of $a^0_{1,11}$ and $a^0_{1,22}$, and the charged states $H^\pm$ are a mixture of $h^\pm_{1,21}$ and $h^\pm_{1,12}$ with an $\mathcal{O}(\xi)$ admixture of $h^\pm_R$.

2. Complete LET model

If we include Φ_2 into the scalar sector, we have 20 real scalar components. These are mixed into six Goldstone bosons, five massive CP-even states, three massive CP-odd states, and three pairs of massive charged scalars. We define the CP-even mass eigenstates h^0, H_1^0, H_2^0, H_3^0, H_4^0, respectively, as the most $h_{1,11}^0$-, $h_{2,11}^0$-, $h_{1,22}^0$-, $h_{2,22}^0$-, h_R^0-like scalars. The massive CP-odd states A_1^0, A_2^0, A_3^0 are defined, respectively, as the most $a_{1,22}^0$-, $a_{2,11}^0$-, a_R^0-like scalars, and the charged states $H_1^\pm$, $H_2^\pm$, $H_3^\pm$ are defined, respectively, as the most $h_{2,21}^\pm$-, $h_{1,12}^\pm$-, $h_{2,12}^\pm$-like scalars. Their masses are found to be

$$\begin{aligned}
\frac{m^2_{h^0,H_1^0}}{v^2} &= \frac{1}{2}\left(\Lambda_1 c_\alpha^2 + \Lambda_2 s_\alpha^2 \pm \sqrt{(\Lambda_1 c_\alpha^2 - \Lambda_2 s_\alpha^2)^2 + \Lambda_3^2 s_{(2\alpha)}^2} + \mathcal{O}(\xi^2)\right)\\
\frac{m^2_{H_2^0}}{M^2} &= \frac{\lambda_5}{2c_{(2\beta_1)}} + \mathcal{O}(\xi^2), \qquad \frac{m^2_{H_3^0}}{M^2} = \frac{\tilde\lambda_4}{2c_{(2\beta_2)}} + \mathcal{O}(\xi^2), \qquad \frac{m^2_{H_4^0}}{M^2} = \lambda_3 + \mathcal{O}(\xi^2),\\
\frac{m^2_{A_1^0}}{v^2} &= -(\tilde\lambda_7 + \tilde\lambda_{10})(c_{\beta_1}^2 c_{\beta_2}^2 + s_{\beta_1}^2 s_{\beta_2}^2) - \frac{\tilde\lambda_6}{2} s_{(2\beta_1)} s_{(2\beta_2)} + \mathcal{O}(\xi^2),\\
\frac{m^2_{A_2^0}}{M^2} &= \frac{\lambda_5}{2c_{(2\beta_1)}} + \mathcal{O}(\xi^2), \qquad \frac{m^2_{A_3^0}}{M^2} = \frac{\tilde\lambda_4}{2c_{(2\beta_2)}} + \mathcal{O}(\xi^2),\\
\frac{m^2_{H_1^\pm}}{v^2} &= -\frac{1}{2}(\tilde\lambda_6 + \tilde\lambda_7 + \tilde\lambda_{10}) c_{(\beta_1-\beta_2)}^2 - \frac{\tilde\lambda_9}{2} c_{(2\beta_1)} c_{(2\beta_2)} + \mathcal{O}(\xi^2),\\
\frac{m^2_{H_2^\pm}}{M^2} &= \frac{\lambda_5}{2c_{(2\beta_1)}} + \mathcal{O}(\xi^2), \qquad \frac{m^2_{H_3^\pm}}{M^2} = \frac{\tilde\lambda_4}{2c_{(2\beta_2)}} + \mathcal{O}(\xi^2).
\end{aligned} \tag{B3}$$

Here we have defined the parameter combinations

$$\begin{aligned}
\Lambda_1 &\equiv \lambda_1 + \lambda_2 c_{\beta_1}^2 - \frac{(\lambda_4 + \lambda_5 s_{\beta_1}^2)^2}{\lambda_3}, \qquad \Lambda_2 \equiv \tilde\lambda_1 + \tilde\lambda_2 c_{\beta_2}^2 - \frac{(\tilde\lambda_3 + \tilde\lambda_4 s_{\beta_2}^2)^2}{\lambda_3},\\
\Lambda_3 &\equiv -\frac{(\lambda_4 + \lambda_5 s_{\beta_1}^2)(\tilde\lambda_3 + \tilde\lambda_4 s_{\beta_2}^2)}{\lambda_3} + \tilde\lambda_5 + (\tilde\lambda_6 + \tilde\lambda_7) c_{(\beta_1-\beta_2)}^2 + (\tilde\lambda_8 + \tilde\lambda_9 + \tilde\lambda_{10})(c_{\beta_1}^2 c_{\beta_2}^2 + s_{\beta_1}^2 s_{\beta_2}^2).
\end{aligned} \tag{B4}$$

APPENDIX C: HIGGS-COUPLING MODIFICATIONS OF THE SB MODEL

The SB model has a larger Higgs sector than the SM. Since the SM-like scalar h^0 is a mixture of the various Higgs fields, its couplings generally differ from those of the SM. These couplings depend on the scalar mixings, which in turn depend on the VEVs and scalar-potential parameters. We give the resulting Higgs-coupling modifications Δ_x, as defined in Eq. (12), in the limit of small ξ. The modifications of the tree-level couplings to W, Z, t, b are given by

$$\begin{aligned}
\frac{\Delta_W}{\xi^2} &= -s_{(2\beta_1)}^2 + \frac{\lambda_2 s_{(4\beta_1)}^2}{8\lambda_5} + \frac{s_{(4\beta_1)} s_{(2\beta_1)} \lambda_{453}}{4} - \frac{s_{\beta_1}^2 \lambda_{453}^2}{2} + \mathcal{O}(\xi),\\
\frac{\Delta_Z}{\xi^2} &= -c_{\theta_W'}^4 + \frac{\lambda_2 s_{(4\beta_1)}^2}{8\lambda_5} + \frac{s_{(4\beta_1)} s_{(2\beta_1)} \lambda_{453}}{4} - \frac{s_{\beta_1}^2 \lambda_{453}^2}{2} + \mathcal{O}(\xi),\\
\frac{\Delta_t}{\xi^2} &= -\frac{2\lambda_2 s_{\beta_1}^2 c_{(2\beta_1)}^2}{\lambda_5} - 2 s_{\beta_1}^2 c_{(2\beta_1)} \lambda_{453} - \frac{\lambda_{453}^2}{2} + \mathcal{O}(\xi^2),\\
\frac{\Delta_b}{\xi^2} &= \frac{2\lambda_2 c_{\beta_1}^2 c_{(2\beta_1)}^2}{\lambda_5} + 2 c_{\beta_1}^2 c_{(2\beta_1)} \lambda_{453} - \frac{\lambda_{453}^2}{2} + \mathcal{O}(\xi^2).
\end{aligned} \tag{C1}$$

Here we defined $\lambda_{453} = (\lambda_4 + \lambda_5 s_{\beta_1}^2)/\lambda_3$. The main contributions to the loop-induced photon coupling of the SM come from the W and t loops. In the SB model, there is an additional contribution from the $H^\pm$ loop:

$$\Delta_\gamma = \frac{\xi^2 A_0(\tau_{H^\pm}) c_{(2\beta_1)}}{A_{\rm SM}\lambda_5}\left(\lambda_1 + \lambda_2\left(1+\frac{1}{2}s^2_{(2\beta_1)}\right) + \lambda_5 c_{(2\beta_1)} - \frac{\lambda_4(\lambda_4+\lambda_5 c^2_{\beta_1})}{\lambda_3} + \mathcal{O}(\xi^2)\right). \quad \text{(C2)}$$

Here $A_s(x)$ are the scalar loop functions, $\tau_x \equiv 4m_x^2/m_{h^0}^2$, and we defined the constant $A_{\rm SM} \equiv A_1(\tau_W) + N_c Q_t^2 A_{1/2}(\tau_t) = -6.5$. The trilinear and quartic Higgs self-couplings are modified as well:

$$\Delta_{\lambda_{3h}} = \frac{-\lambda_2\lambda_3 s^2_{\beta_1} c_{(2\beta_1)}}{\lambda_3(\lambda_1+\lambda_2 c^2_{\beta_1}) - (\lambda_4+\lambda_5 s^2_{\beta_1})^2} + \mathcal{O}(\xi^2),$$
$$\Delta_{\lambda_{4h}} = \frac{-\lambda_2\lambda_3 s^2_{\beta_1} c_{(2\beta_1)} + (\lambda_4+\lambda_5 s^2_{\beta_1})^2}{\lambda_3(\lambda_1+\lambda_2 c^2_{\beta_1}) - (\lambda_4+\lambda_5 s^2_{\beta_1})^2} + \mathcal{O}(\xi^2). \quad \text{(C3)}$$

Note that the coupling modifications for vector bosons and fermions vanish in the small-ξ limit, that is, the new physics decouples from the SM. However, the modifications of the Higgs self-couplings only vanish for the region of parameter space where $\lambda_2 = 0$ and $\lambda_4 = -\lambda_5 s^2_{\beta_1}$. In general, the self-couplings are modified due to the more complicated structure of the scalar potential.

If we look for regions of parameter space where the coupling modifications become substantial, it is more useful to write the coupling modifications in terms of the scalar mixing coefficients a_i, as defined in Eq. (14):

$$\Delta_{W,Z} = c_{\beta_1} a_1 + s_{\beta_1} a_2 - 1 + \mathcal{O}(\xi^2),$$
$$\Delta_t = a_1/c_{\beta_1} - 1,$$
$$\Delta_b = a_2/s_{\beta_1} - 1. \quad \text{(C4)}$$

The analogous coupling modifications $\Delta_x^{\rm FP}$ of H_2^0 are obtained by substituting each a_i by $a_i^{\rm FP}$. Since $\beta_1 = 0.0166$ is small, we can write $\Delta_W = \Delta_Z = \Delta_t \equiv \Delta_1$ and $\Delta_{W,Z}^{\rm FP} = \Delta_t^{\rm FP} \equiv \Delta_1^{\rm FP}$, up to $\mathcal{O}(\xi^2)$ and $\mathcal{O}(\beta_1)$ corrections.

[1] G. Aad *et al.* (ATLAS Collaboration), Phys. Lett. B **716**, 1 (2012).
[2] S. Chatrchyan *et al.* (CMS Collaboration), Phys. Lett. B **716**, 30 (2012).
[3] M. Baak and R. Kogler, arXiv:1306.0571.
[4] H. Georgi and S. Glashow, Phys. Rev. Lett. **32**, 438 (1974).
[5] H. Fritzsch and P. Minkowski, Ann. Phys. (N.Y.) **93**, 193 (1975).
[6] F. Gursey, P. Ramond, and P. Sikivie, Phys. Lett. B **60**, 177 (1976).
[7] Y. Achiman and B. Stech, Phys. Lett. B **77**, 389 (1978).
[8] Q. Shafi, Phys. Lett. B **79**, 301 (1978).
[9] P. Candelas, G. T. Horowitz, A. Strominger, and E. Witten, Nucl. Phys. **B258**, 46 (1985).
[10] E. Witten, Nucl. Phys. **B258**, 75 (1985).
[11] E. Cremmer, J. Scherk, and J. H. Schwarz, Phys. Lett. B **84**, 83 (1979).
[12] K. S. Babu, X.-G. He, and S. Pakvasa, Phys. Rev. D **33**, 763 (1986).
[13] X.-G. He and S. Pakvasa, Phys. Lett. B **173**, 159 (1986).
[14] G. Lazarides and C. Panagiotakopoulos, Phys. Lett. B **336**, 190 (1994).
[15] G. Lazarides and C. Panagiotakopoulos, Phys. Rev. D **51**, 2486 (1995).
[16] A. Demaria and R. R. Volkas, Phys. Rev. D **71**, 105011 (2005).
[17] C. Cauet, H. Päs, and S. Wiesenfeldt, Phys. Rev. D **83**, 093008 (2011).
[18] J. Sayre, S. Wiesenfeldt, and S. Willenbrock, Phys. Rev. D **73**, 035013 (2006).
[19] B. Stech and Z. Tavartkiladze, Phys. Rev. D **70**, 035002 (2004).
[20] B. Stech and Z. Tavartkiladze, Phys. Rev. D **77**, 076009 (2008).
[21] B. Stech, arXiv:1012.6028.
[22] B. Stech, Phys. Rev. D **86**, 055003 (2012).
[23] B. Stech, J. High Energy Phys. 08 (2014) 139.
[24] J. C. Pati and A. Salam, Phys. Rev. D **10**, 275 (1974).
[25] R. N. Mohapatra and J. C. Pati, Phys. Rev. D **11**, 566 (1975).
[26] G. Senjanovic and R. N. Mohapatra, Phys. Rev. D **12**, 1502 (1975).
[27] T. Lee, Phys. Rev. D **8**, 1226 (1973).
[28] The matrices $G_{\alpha\beta}$ and $A_{\alpha\beta}$ can be viewed, respectively, as the real and imaginary components of the VEV of a flavon field (see Ref. [20]). In this picture, the Yukawa interactions are effective interactions arising from dimension-five operators, which in turn arise from interactions with gauge-singlet fermions. However, the components of these matrices are simply considered as free parameters of the trinification model.
[29] G. Branco, P. Ferreira, L. Lavoura, M. Rebelo, M. Sher, and J. P. Silva, Phys. Rep. **516**, 1 (2012).
[30] S. P. Martin, Adv. Ser. Dir. High Energy Phys. **21**, 1 (2010).
[31] D. B. Kaplan, H. Georgi, and S. Dimopoulos, Phys. Lett. B **136**, 187 (1984).
[32] N. Arkani-Hamed, A. G. Cohen, and H. Georgi, Phys. Lett. B **513**, 232 (2001).
[33] Note that other models allow for the existence of a light fermiophobic Higgs as well, such as the type-I 2HDM and models with $SU(2)_L$-triplet Higgs fields [44–46]. However, in those scenarios the light Higgs h^0 is fermiophobic, whereas we consider benchmark scenarios with a fermiophobic light Higgs *in addition to* the SM-like Higgs.

[34] Our use of the term "twin Higgs" is not to be confused with "twin Higgs models" in the literature. In those models, each Standard Model particle has a corresponding particle that transforms under a mirror copy of the SM gauge group (see e.g. Refs. [65,66]). The copies are related by a Z_2 symmetry called "twin parity," and the twin Higgs is the partner of the Standard Model Higgs.
[35] B. Stech, arXiv:1303.6931.
[36] M. Heikinheimo, A. Racioppi, M. Raidal, and C. Spethmann, Phys. Lett. B **726**, 781 (2013).
[37] A. Barroso, P. Ferreira, and R. Santos, Phys. Lett. B **652**, 181 (2007).
[38] Wolfram Research, Inc., Mathematica, Version 10.0, Champaign, Illinois, 2014.
[39] D. López-Val, T. Plehn, and M. Rauch, J. High Energy Phys. 10 (2013) 134.
[40] R. Lafaye, T. Plehn, M. Rauch, D. Zerwas, and M. Duhrssen, J. High Energy Phys. 08 (2009) 009.
[41] M. Klute, R. Lafaye, T. Plehn, M. Rauch, and D. Zerwas, Phys. Rev. Lett. **109**, 101801 (2012).
[42] T. Plehn and M. Rauch, Europhys. Lett. **100**, 11002 (2012).
[43] P. Osland, P. N. Pandita, and L. Selbuz, Phys. Rev. D **78**, 015003 (2008).
[44] A. Akeroyd, Phys. Lett. B **368**, 89 (1996).
[45] J. F. Gunion, R. Vega, and J. Wudka, Phys. Rev. D **42**, 1673 (1990).
[46] P. Bamert and Z. Kunszt, Phys. Lett. B **306**, 335 (1993).
[47] K. Olive *et al.* (Particle Data Group), Chin. Phys. C **38**, 090001 (2014).
[48] P. Abreu *et al.* (DELPHI Collaboration), Phys. Lett. B **507**, 89 (2001).
[49] A. Heister *et al.* (ALEPH Collaboration), Phys. Lett. B **544**, 16 (2002).
[50] P. Achard *et al.* (L3 Collaboration), Phys. Lett. B **534**, 28 (2002).
[51] G. Abbiendi *et al.* (OPAL Collaboration), Phys. Lett. B **544**, 44 (2002).
[52] G. Aad *et al.* (ATLAS Collaboration), Eur. Phys. J. C **72**, 2157 (2012).
[53] S. Chatrchyan *et al.* (CMS Collaboration), Phys. Lett. B **725**, 36 (2013).
[54] S. Chatrchyan *et al.* (CMS Collaboration), J. High Energy Phys. 09 (2012) 111.
[55] G. Aad *et al.* (ATLAS Collaboration), Phys. Lett. B **726**, 88 (2013).
[56] S. Chatrchyan *et al.* (CMS Collaboration), J. High Energy Phys. 05 (2014) 104.
[57] S. Dittmaier *et al.* (LHC Higgs Cross Section Working Group), Report No. CERN-2011-002.
[58] A. Djouadi, J. Kalinowski, and M. Spira, Comput. Phys. Commun. **108**, 56 (1998).
[59] F. Abe *et al.* (CDF Collaboration), Phys. Rev. Lett. **79**, 2192 (1997); G. Abbiendi *et al.* (OPAL Collaboration), Eur. Phys. J. Spec. Top. **C33**, 173 (2004); J. Abdallah *et al.* (DELPHI Collaboration), Eur. Phys. J. C **45**, 589 (2006); S. Schael *et al.* (ALEPH Collaboration), Eur. Phys. J. C **49**, 411 (2007); G. Aad *et al.* (ATLAS Collaboration), Eur. Phys. J. C **72**, 2241 (2012); Phys. Rev. Lett. **109**, 081801 (2012); Phys. Lett. B **719**, 242 (2013); J. High Energy Phys. 11 (2012) 138; Phys. Rev. D **85**, 112012 (2012); S. Chatrchyan *et al.* (CMS Collaboration), Phys. Lett. B **718**, 1229 (2013); Phys. Rev. Lett. **109**, 141801 (2012); Phys. Lett. B **720**, 63 (2013); J. High Energy Phys. 02 (2013) 036; 01 (2013) 013; G. Aad *et al.* (ATLAS Collaboration), Phys. Rev. D **87**, 112006 (2013); S. Chatrchyan *et al.* (CMS Collaboration), Phys. Rev. D **87**, 072005 (2013).
[60] J. Chay, K. Y. Lee, and S.-h. Nam, Phys. Rev. D **61**, 035002 (1999).
[61] F. del Aguila, J. de Blas, and M. Perez-Victoria, J. High Energy Phys. 09 (2010) 033.
[62] G. Barenboim, J. Bernabeu, J. Prades, and M. Raidal, Phys. Rev. D **55**, 4213 (1997).
[63] J. Bueno *et al.* (TWIST Collaboration), Phys. Rev. D **84**, 032005 (2011).
[64] A. Hillairet *et al.* (TWIST Collaboration), Phys. Rev. D **85**, 092013 (2012).
[65] Z. Chacko, H.-S. Goh, and R. Harnik, Phys. Rev. Lett. **96**, 231802 (2006).
[66] Z. Chacko, Y. Nomura, M. Papucci, and G. Perez, J. High Energy Phys. 01 (2006) 126.